Electronic Supplementary Material (ESI) for Environmental Science: Nano.

Supplementary Information

RGO-Functionalized Polymer Nanofibrous Membrane with Exceptional Surface Activity and Ultra-Low Airflow Resistance for $PM_{2.5}$ Filtration

Peng Zhang,[abc] Dongyang Wan,[ab] Zhenyi Zhang,*[abd] Guodong Wang,[e] Junhua Hu[abc] and Guosheng Shao[abc]

[a] *School of Materials Science and Engineering, Zhengzhou University, Zhengzhou 450001, P. R. China*

[b] *State Centre for International Cooperation on Designer Low-Carbon & Environmental Materials (CDLCEM), Zhengzhou University, Zhengzhou 450001, P. R. China*

[c] *Zhengzhou Materials Genome Institute, Xingyang 450100, P. R. China.*

[d] *Key Laboratory of New Energy and Rare Earth Resource Utilization of State Ethnic Affairs Commission, Key Laboratory of Photosensitive Materials and Devices of Liaoning Province, School of Physics and Materials Engineering, Dalian Nationalities University, 18 Liaohe West Road, Dalian 116600, P. R. China; E-mail:* zhangzy@dlnu.edu.cn

[e] *Dalian Juyang Technology Co.,Ltd, Dalian 116085, P. R. China*

1. Experimental

1.1 Electrospinning fabrication of the polyacrylonitrile (PAN) and the reduced graphene oxide (rGO)-functionalized PAN nanofibrous membranes (NFMs):

Firstly, 0.48 g of PAN powder (Mw = 150,000) and a certain amount of rGO nanosheets (NSs) were added into 8 mL of DMF solution under vigorous stirring for 24 h to form a rGO NSs-suspended solution. The rGO nanosheets were provided by the Zhengzhou New Century Materials Genome Institute (ZMGI) according to a latest invention [CN201710161814.7]. Subsequently, the above precursor solution was put into a 10-mL syringe for electrospinning during which a 10-kV high-voltage was applied, and the working distance between the electrospun needle and collector was fixed at ~15 cm. Finally, the rGO/PAN composite nanofibers were obtained on the collector, which then interweaved the rGO-functionalized PAN NFMs. The weight ratios of rGO NSs to PAN were 0, 1.0, 2.5, 5.0, and 10.0 wt. %, respectively.

1.2 Characterization:

The morphologies of the as-fabricated samples were observed under the field emission scanning electron microscopy (FESEM, JSM-7500F) and transmission electron microscope (TEM, FEI Tecnai G2 F20). The crystallization of the as-fabricated samples were identified by the X-ray diffraction (XRD) (Rigaku Ultima IV) with Cu Kα radiation (λ=0.15406 nm) from 10° to 80°. The X-ray photoelectron spectroscopy (XPS) was measured by using the multifunctional X-ray photoelectron spectroscopy (AXIS UltraDLD, Kratos Analytical Inc). Raman spectra were performed on a Jobin-Yvon HR800 micro-Raman spectrometer using the 488 nm line of a He–Cd laser as the excitation source at room temperature. The mechanical properties of the as-electrospun NFMs were measured under the tensile mode through an universal materials testing machine (SHIMADZU, AG-I 20KN). The stress-strain curves of the NFMs were obtained through the calculation of the primary data. The calculation method is the same to the literature (ACS Nano, 2015, 9, 9292), during which the whole-structure effect of the NFMs could be normalized to directly compare the mechanical properties of electrospun nanofibers.

1.3 $PM_{2.5}$ filtration measurements:

The model of PM pollution was constructed by burning the mosquito repellent incense or

the cigarette during the performance tests. The inflow concentration was controlled by diluting to a hazardous pollution level equivalent to the $PM_{2.5}$ index > 300. PM particle number concentration was detected with and without filters by a particle counter range of 0-500μg/m^3 (CEM, DT-9881M) and the removal efficiency was calculated by comparing the number concentration before and after filtration. The pressure drop was measured by a differential pressure gauge (CEM, 8920).

1.4 Theoretical calculations:

All electronic structure calculations were carried out with the Gaussian 09 program suite.[1] Geometry optimizations of all complexes were implemented using DFT method, and the Becke's three-parameter hybrid exchange functional with Lee−Yang−Parr gradient-corrected correlation (B3LYP functional) and 6-311g(d,p) basis set [2-4] is employed in the calculations. The frequency calculations on optimized geometries were also performed to verify that they correspond to local minima on the energy surfaces.

1. M. J. Frisch, G. W. Trucks, H. B. Schlegel, G. E. Scuseria, M. A. Robb, J. R. Cheeseman, G. Scalmani, V. Barone, B. Mennucci, G. A. Petersson, H. Nakatsuji, M. Caricato, X. Li, H. P. Hratchian, A. F. Izmaylov, J. Bloino, G. Zheng, J. L. Sonnenberg, M. Hada, M. Ehara, K. Toyota, R. Fukuda, J. Hasegawa, M. Ishida, T. Nakajima, Y. Honda, O. Kitao, H. Nakai, T. Vreven, J. A. Montgomery, Jr, J. E. Peralta, F. Ogliaro, M. Bearpark, J. J. Heyd, E. Brothers, K. N. Kudin, V. N. Staroverov, R. Kobayashi, J. Normand, K. Raghavachari, A. Rendell, J. C. Burant, S. S. Iyengar, J. Tomasi, M. Cossi, N. Rega, J. M. Millam, M. Klene, J. E. Knox, J. B. Cross, V. Bakken, C. Adamo, J. Jaramillo, R. Gomperts, R. E. Stratmann, O. Yazyev, A. J. Austin, R. Cammi, C. Pomelli, J. W. Ochterski, R. L. Martin, K. Morokuma, V. G. Zakrzewski, G. A. Voth, P. Salvador, J. J.Dannenberg, S. Dapprich, A. D. Daniels, O. Farkas, J. B. Foresman, J. V. Ortiz, J. Cioslowski and D. J. Fox, Gaussian 09, Revision A.02, Gaussian, Inc., Wallingford CT, 2009.
2. C. T. Lee, W. T. Yang and R. G. Parr, Phys. Rev. B: Condens. Matter Mater. Phys., 1988, 37, 785.
3. B. Miehlich, A. Savin, H. Stoll and H. Preuss, Chem. Phys. Lett., 1989, 157, 200.
4. A. D. Becke, J. Chem. Phys., 1993, 98, 5648.

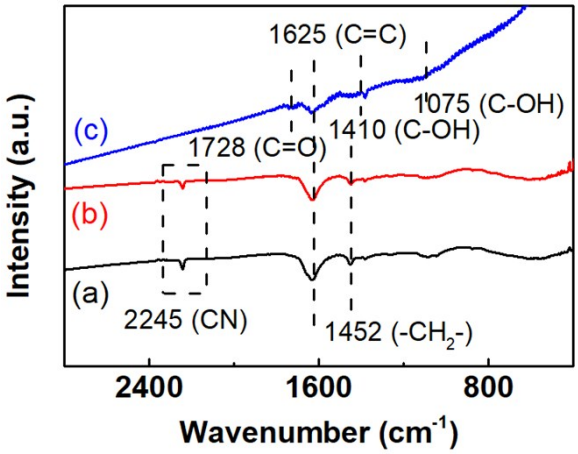

Figure S1 FT-IR spectra of (a) PAN NFM, (b) 2.5 wt.% rGO-functionalized PAN NFM, and (c) rGO NSs.

The FT-IR spectrum of rGO NSs indicates the presence of C=O (1728 cm^{-1}) from stretching vibrations of carbonyl and carboxylic groups, C−OH (1410 and 1075 cm^{-1}) from the stretching vibration of hydroxyl, and C=C/C-C (1625 cm^{-1}) from the stretching vibration of graphitic domains, which confirms the presence of oxygen-containing functional groups on the rGO surface. Meanwhile, the spectrum of PAN nanofibers presents the stretching C ≡ N bond vibration at 2245 cm^{-1} and the strong deformation vibration of -CH_2- group at 1452 cm^{-1}, which are both characteristic vibrations of PAN. However, after introducing the rGO NSs into the PAN nanofibers, we could only observe the characteristic vibrations of PAN on the FT-IR spectrum of 2.5 wt.% rGO/PAN composite nanofibers. The lack of FT-IR signal for rGO NSs can be attributed to the low content and good dispersion of rGO NSs in the composite nanofibers.

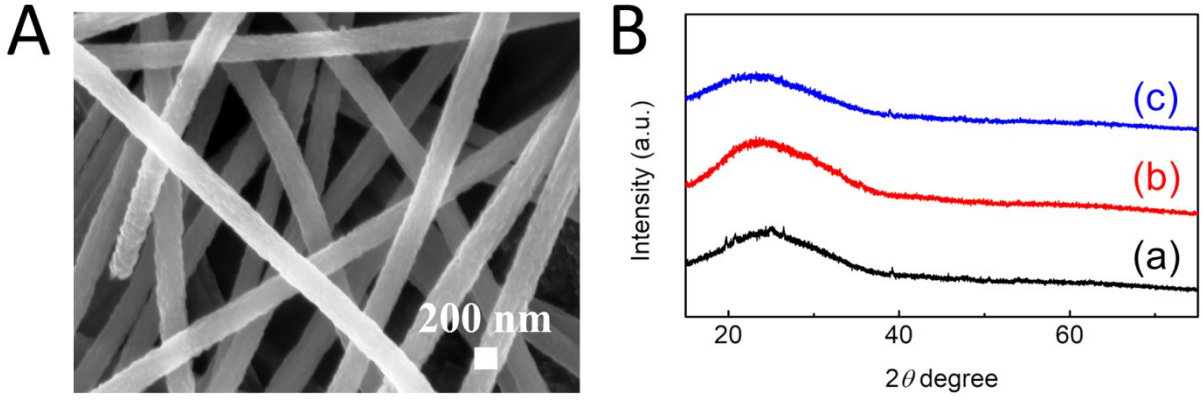

Figure S2 (A) SEM image of as-electrospun PAN nanofibers; (B) XRD patterns of the as-electrospun rGO-functionalized PAN NFMs with the rGO content of (a) 1.0 wt.%, (b) 5.0 wt.%, and (c) 10.0 wt.%.

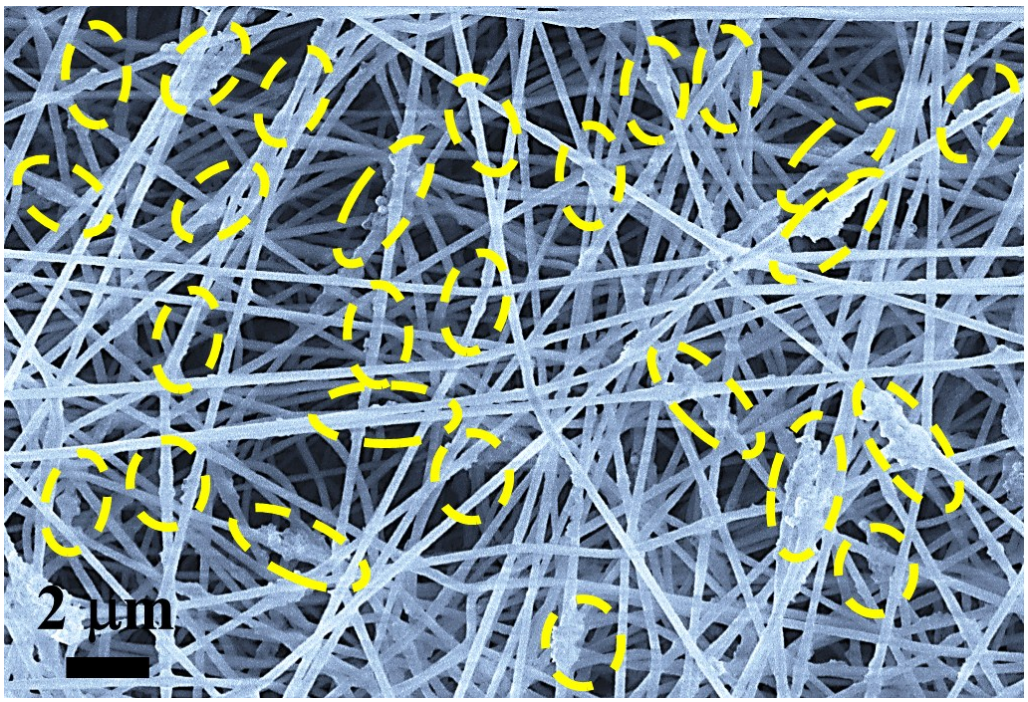

Figure S3 SEM image of the 2.5 wt.% rGO/PAN composite nanofibers with the marked rGO NSs components.

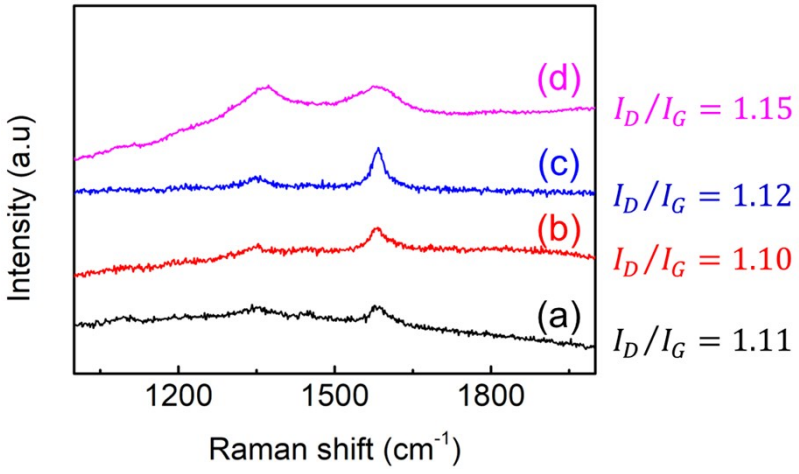

Figure S4 Raman spectra of the as-electrospun rGO-functionalized PAN NFMs with the rGO content of (a) 1.0 wt.%, (b) 2.5 wt.%, (c) 5.0 wt.%, and (d) 10.0 wt.%.